

# Generation of attosecond x-ray pulses beyond the atomic unit of time using laser induced microbunching in electron beams\*

D. Xiang<sup>†</sup>, Z. Huang and G. Stupakov, SLAC, Menlo Park, CA 94025 USA

## Abstract

Ever since the discovery of mode-locking, efforts have been devoted to reducing the duration of laser pulses since the ultrashort pulses are critical to explore the dynamics occurred on a ever-shorter timescale. In this paper we describe a scheme that's capable of generating intense attosecond x-ray pulses with duration beyond the atomic unit of time ( $\sim 24$  attoseconds). The scheme combines the echo-enabled harmonic generation technique with the bunch compression which allows one to generate harmonic numbers of a few hundred in a microbunched beam through up-conversion of the frequency of a UV seed laser. A few-cycle intense IR laser is used to generate the required energy chirp in the beam for bunch compression and for selection of an attosecond x-ray pulse. Using a representative realistic set of parameters, we show that 1 nm x-ray pulse with peak power of a few hundred MW and duration as short as 20 attoseconds (FWHM) can be generated from a 200 nm UV seed laser. The proposed scheme may enable the study of electronic dynamics with a resolution beyond the atomic unit of time and may open a new regime of ultrafast sciences.

## INTRODUCTION

Fast time-dependent phenomena are typically studied with pump-probe technique in which the dynamics are initiated by a pump laser and then probed by a delayed pulse. The temporal resolution depends on the duration of the pump and probe beams. The advent of attosecond (as) pulses made possible the time-resolved study of the electronic dynamics which opened up many new ultrafast sciences [1-5]. Using the  $\sim 100$  as soft x-ray pulse in the wavelength  $\sim 10$  nm, the light wave was measured in [2] and the electron tunneling in atoms was observed in [3]. Most recently the pulse duration has been pushed to about 80 as in the extreme ultraviolet wavelength [5]. These studies all relied on the technique of high harmonic generation in gas where an intense laser pulse was focused on an atomic gas jet and the high harmonic of the laser was generated and further used as the probe. However, it appears difficult to generate intense harmonic radiation with wavelength down to 1 nm or shorter with this technique.

To achieve atomic spatial resolution, the radiation wavelength needs to be pushed to  $\sim 1$  nm or shorter, and the isolated attosecond pulse is also highly desirable. There is a growing trend to provide such attosecond x-ray pulses using free electron lasers (FEL) [6-17]. Most of the proposed

schemes utilized intense lasers to manipulate the electron beam energy and then selected a small part of the electrons to lase [8-13,16-17]. The schemes [7,9-14] that use self-amplified spontaneous emission (SASE) to generate attosecond x-ray pulse may suffer from statistic fluctuations because SASE originates from electron beam shot noise. An alternative scheme [8] which overcomes this problem is to use the high-gain harmonic generation (HG) configuration. But due to the relatively low up-frequency conversion efficiency, the HG scheme requires an intense seed signal in the wavelength of a few nm which is in principle obtainable but does not exist today.

In this paper, we describe a novel scheme [16] which allows generation of intense isolated attosecond x-ray in the wavelength  $\sim 1$  nm or shorter based on existed technologies. The scheme combines the echo-enabled harmonic generation (EEHG) technique [18,19] with the bunch compression technique and allows harmonic numbers of a few hundred to be accessible that eventually enables the generation of x-ray radiation from a UV seed laser. The required energy chirp in the bunch compression is provided by a few-cycle intense IR laser which finally assists in selection of an isolated attosecond x-ray pulse. Using a representative realistic set of parameters, we show that 1 nm isolated x-ray pulse with duration of about 20 as (FWHM) and peak power of about 180 MW can be generated in a short radiator with only 12 undulator periods using the proposed scheme. Since the generated attosecond x-ray pulse is in tight synchronization with the few-cycle laser, it is straightforward to use them for ultrafast pump-probe experiments. The proposed scheme may enable the study of electronic dynamics with a resolution beyond the atomic unit of time ( $\sim 24$  as) and may open a new regime of ultrafast sciences.

## METHODS

Our scheme requires an ultrarelativistic electron beam, a UV seed laser, a few-cycle intense IR laser, together with four undulator sections and two dispersion sections. The wavelength of the UV seed laser is assumed to be 200 nm and that of the few-cycle IR laser is 800 nm. We further assume that the lasers originate from the same Ti:Sapphire oscillator which will allow tight synchronization between them. The schematic of the proposed scheme is shown in Fig. 1.

The first part of the proposed scheme is similar to the EEHG FEL [18,19] in which the beam is energy modulated in the first modulator (M1) and then sent through a dispersion section with strong dispersion strength  $R_{56}^{(1)}$  after which the modulation obtained in M1 is macroscopically washed out while simultaneously complicated fine

\* Work supported by US DOE contracts DE-AC02-76SF00515.

<sup>†</sup> dxiang@slac.stanford.edu

structures (separated energy bands) are introduced into the phase space. In the EEHG scheme, a second laser is used to further modulate the beam energy in the second modulator (M2). After passing through the second dispersion section with dispersion strength  $R_{56}^{(2)}$ , the separated energy bands will convert to separated current bands and the echo signal then occurs as a recoreherence effect caused by the mixing of the correlations between the modulation in the second modulator and the fine structures.

In our proposed scheme for generation of an attosecond x-ray pulse, we introduce an extra modulator (M3) between M2 and the second dispersion section. The beam interacts in M3 with a few-cycle intense laser of which the wavelength is chosen to be much longer than that of the laser in M2, so that part of the electrons around the zero crossing of the few-cycle laser gets almost linear energy chirp. With this additional energy chirp, the beam is longitudinally compressed after passing through the second dispersion section and the harmonic number is increased by the compression factor. As we will show below, in addition to assisting in extension of the harmonic number to a few hundred, the few-cycle laser also offers a possibility to select an isolated attosecond pulse.

We assume an initial Gaussian beam energy distribution with an average energy  $E_0$  and the rms energy spread  $\sigma_E$ , and use the variable  $p = (E - E_0)/\sigma_E$  for the dimensionless energy deviation of a particle. The initial normalized distribution function of the beam is  $f_0(p) = N(2\pi)^{-1/2}e^{-p^2/2}$ , where  $N$  is the number of electrons per unit length of the beam. The beam energy is modulated with the amplitude  $\Delta E_1$  in M1, and the distribution function after beam passing through the first dispersion section with the dispersion strength  $R_{56}^{(1)}$  is [18,19],

$$f_1(\zeta, p) = \frac{N}{\sqrt{2\pi}} \exp \left[ -\frac{1}{2} (p - A_1 \sin(\zeta - B_1 p))^2 \right], \quad (1)$$

where  $A_1 = \Delta E_1/\sigma_E$ ,  $\zeta = kz$ ,  $z$  is the longitudinal coordinate in the beam,  $k$  is the wave number of the laser and  $B_1 = R_{56}^{(1)}k\sigma_E/E_0$ . The beam is then energy modulated in M2 with the dimensionless modulation amplitude  $A_2$ . After modulation in M2, the beam is further energy modulated in M3 with an intense, few-cycle laser for which the wavelength is much longer than that in the upstream modulators. The carrier-envelope phase of the few-cycle laser pulse is set to  $\pi/2$  so that the oscillating electric field is

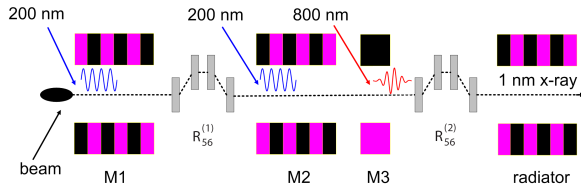


Figure 1: Schematic of the proposed scheme for generation of isolated attosecond x-ray pulse.

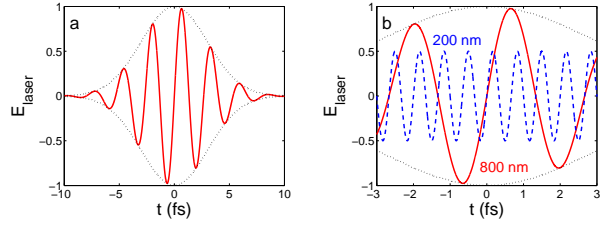


Figure 2: (a) A snapshot of the laser field normalized to the peak value for the 800 nm few-cycle laser with pulse length 5 fs (FWHM of intensity); (b) Schematic of the synchronization between the laser in M2 and the few-cycle laser (laser field not in scale).

zero at the pulse peak [20]. A snapshot of the 800 nm few-cycle laser field normalized to the peak value is shown in Fig. 2a.

To show how the few-cycle laser assists in generation of much higher harmonic and an attosecond x-ray pulse, we add a linear energy chirp to the beam distribution before sending the beam to the second dispersion section. Assuming the linear energy chirp factor is  $h = dp/d\zeta$ , the resulting longitudinal phase space distribution at the exit from the second dispersion section is,

$$f_2(\zeta, p) = \frac{N}{\sqrt{2\pi}} \exp \left[ -\frac{1}{2} \left( (1 + hB_2)p - h\zeta - A_2 \sin(\zeta - B_2 p) - A_1 \sin[(1 + hB_1)\zeta + A_2 B_1 \sin(\zeta - B_2 p) - (B_1 + B_2 + hB_1 B_2)p] \right)^2 \right], \quad (2)$$

where  $B_2 = R_{56}^{(2)}k\sigma_E/E_0$ . Integration of Eq. (2) over  $p$  yields the final current distribution which can be expanded in Fourier series,

$$b(\zeta) = CN \left[ 1 + 2 \sum_{n=1}^{\infty} b_n \cos(Cn\zeta + \psi_n) \right], \quad (3)$$

The wave number of the echo signal is  $Cnk$ , where  $C = 1/(1 + hB_2)$  is the compression factor and the corresponding maximized bunching factor for this harmonic radiation is,

$$b_n = |J_{n+1}(CnA_2B_2) J_1(A_1(CnB_2 - B_1))| \exp \left[ -\frac{1}{2} (CnB_2 - B_1)^2 \right], \quad (4)$$

The bunching factor at the harmonic number  $m$  is defined as  $\langle e^{imkz} \rangle$ , where  $mk$  is the wave number of the harmonic radiation and the brackets denote averaging over the longitudinal coordinate  $z$ . A comparison between this equation and Eq. (6) in Ref. [19] indicates that for given energy modulation amplitudes the bunch compression extends the harmonic number by a factor of  $C$  while keeping the value of the bunching factor unchanged.

## GENERATION OF AN ISOLATED ATTOSECOND X-RAY PULSE

To show the feasibility of the proposed scheme in generating an attosecond x-ray pulse, we consider a representative set of parameters:  $E = 3$  GeV,  $I = 1$  kA,  $\epsilon_n = 1$  mm mrad. A 200 nm laser with peak power  $\sim 100$  MW is used to modulate the beam in M1 and M2 with the peak-to-peak energy modulation amplitude of 900 keV which corresponds to  $A_1 = A_2 = 3$ . Assuming a compression factor of 10, the optimized dispersion strengths and the chirp factor which maximize the bunching factor of the 200th harmonic ( $n = 20$ ,  $C = 10$ ) are found to be  $B_1 \approx 7.213$ ,  $B_2 \approx 0.039$  and  $h \approx -23.241$ , respectively. With these parameters, the electrons are tracked through the modulators and dispersion sections with our 1-D code and the bunching factors for the 200th harmonic (1 nm wavelength for a 200 nm seeding laser) is found to be about 0.12. Sending this prebunched beam to the radiator will generate powerful coherent x-ray at 1 nm wavelength.

To generate an isolated attosecond x-ray pulse, an 800 nm few-cycle laser with energy  $\sim 1$  mJ and pulse length of 5 fs (FWHM) is used to modulate the beam in M3. This kind of laser has been demonstrated with current technologies [4,20]. To take advantage of the bunch compression assisted harmonic generation, the few-cycle laser is time delayed to make its zero crossing overlap with that of the UV laser in M2, as is shown in Fig. 2b. Because the wavelength of the few-cycle laser is much longer than that of the UV laser in M2, the electrons in the regions around the zero crossings get almost linear energy chirp which allows longitudinal compression after passing through a dispersive element. The longitudinal phase space of the beam after interaction with the few-cycle laser is simulated with our 1-D code and shown in Fig. 3.

From Fig. 3 it follows that there are three regions where electrons have almost linear negative energy chirp: the region around the zero crossing of the central cycle ( $t = 0$ , region 1 in Fig. 3) and those around the zero crossings of the nearest side cycles ( $t = \pm 2.67$  fs, region 2 and 3 in Fig. 3). It can be easily seen that the energy chirp factor for the electrons in region 2 and region 3 are approximately 1.5 times smaller than those in region 1. The laser power is adjusted in such a way that only electrons in region 1 have the correct chirp factor ( $h \approx -23.241$ ) to maximize the 200th harmonic of the seed laser. In this case only the separated energy bands in the central cycle are effectively converted to separated current bands which contain considerable higher harmonic components while those in the side cycles fail to convert to 'upright' bands due to the small chirp factor. The bunching factor at 1 nm wavelength for the central slice is about 0.12 and that for all other slices is at the shot noise level, which makes possible the generation of an isolated attosecond x-ray pulse. The current of the central slice is also enhanced by a factor of 10 from the bunch compression. It can be expected that intense 1 nm x-rays will be generated after sending this prebunched, high-

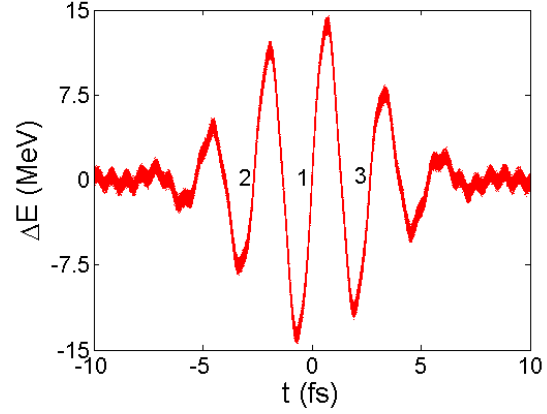


Figure 3: Longitudinal phase space of the beam after interaction with the few-cycle laser (bunch head at left).

peak-current beam slice through the radiator. The output radiation field may be calculated by summing up the field of each electron in the radiator. The output x-ray pulse length is determined by both the electron bunch length and the slippage length in the undulator. For the SASE schemes [7,9-14], the slippage length associated with the long FEL undulator typically limits the radiation pulse length to a few hundred attoseconds. Since in our scheme a short section of the beam is effectively prebunched at the radiator entrance, only a short undulator is required to generate intense coherent x-ray radiation which may allow pushing the pulse duration to below the atomic unit of time ( $\sim 24$  as). In our example, we used a planar undulator with  $N_u = 12$  periods and the period length  $\lambda_u = 4$  cm to generate  $\lambda_r = 1$  nm x-rays. We further assumed that the relative longitudinal position of the electrons did not change during the passage through the short radiator (i.e. no FEL interaction), which was justified for an electron beam with  $1 \mu\text{m}$  normalized emittance and a transverse rms size  $\sigma_x = 20 \mu\text{m}$ . For these parameters, the single-electron undulator radiation has a rms transverse size  $\sqrt{2\lambda_r\lambda_u N_u}/(4\pi) \ll \sigma_x$  and can be approximated as a plane wave. Thus the output power can be calculated as (see for example [21])

$$P(t) = \frac{e^2 c^2 Z_0 K^2 [JJ]^2 \lambda_u^2}{32\pi \sigma_x^2 \gamma_0^2 \lambda_r^2} \left| \sum_j e^{-i2\pi c(t_j - t)/\lambda_r} \right|^2, \quad (5)$$

where  $Z_0 = 377 \Omega$  is the vacuum impedance,  $[JJ] = J_0(\xi) - J_1(\xi)$  is the usual Bessel function factor associated with the planar undulator,  $\xi = K^2/(4 + 2K^2)$ ,  $E_0 = \gamma_0 m c^2$  is the beam energy, and the sum over  $j$ th electron is carried out within the radiation slippage length, i.e.  $0 < c(t_j - t) < N_u \lambda_r$ . Using the beam distribution at the radiator entrance, the power profile of the x-ray radiation at 1 nm wavelength generated in the radiator is shown in Fig. 4. The peak power is about 180 MW, and the pulse length is about 20 as (FWHM), shorter than the atomic unit of time. The number of photons contained in this pulse is about  $2.4 \times 10^7$ .

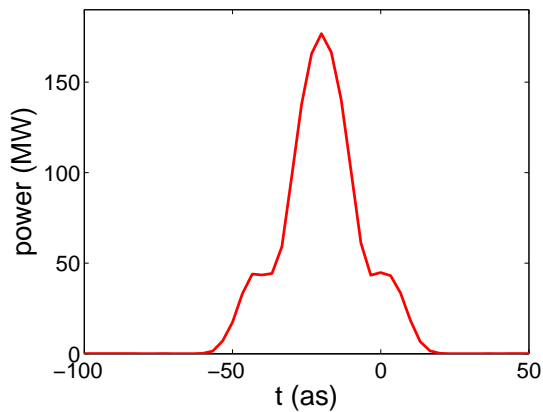


Figure 4: Power of the generated 1 nm x-ray pulse. The pulse length is 20 as (FWHM).

## GENERATION OF TWO ATTOSECOND PULSES

In addition to generation of an isolated intense attosecond x-ray pulse to implement the optical-pump x-ray probe experiment, the proposed scheme may also be used to generate two attosecond x-ray pulses with adjustable delay which may have applications in single color x-ray pump-probe experiments.

In the section above, the laser power is adjusted in such a way that only the central slice of the beam has the correct chirp to maximize the bunching factor. In order to generate two attosecond pulses, one can adjust laser power to make the nearest side slices have the correct chirp while the central slice and other slice has larger or smaller chirp, so that after the dispersion section only the nearest side slices are effectively bunched while the central slice and other slices are either over-bunched or under-bunched. In this case one can generate two attosecond x-ray pulses of which the delay is 2 times the IR laser wavelength (5.3 fs).

To provide adjustable delay between the two pulses, one may use an IR laser with a longer duration. For instance, one may use a commercially available 800 nm laser with FWHM duration of 25 fs in M3. In this case by properly choosing the laser power and dispersion strength, in principle two attosecond x-ray pulses with adjustable delay in the range from 5.3 fs to the duration of the IR laser can be generated. However, it should be pointed out that the delay time between the pulses will be an integer of 5.3 fs. Recently a scheme to generate two attosecond x-ray pulses with different carrier frequency and flexible delay has been proposed in Ref. [17].

## CONCLUSIONS

In conclusion, we have described a scheme that combines the EEHG technique with bunch compression which extends the harmonic numbers to a few hundred. The required energy chirp is generated using a few-cycle intense

laser which also assists in selection of an isolated attosecond x-ray pulse. We emphasize that this pulse is only generated due to created microstructures in the beam, and does not involve additional bunching due to the FEL interaction. Using a representative realistic set of parameters we have shown that 1 nm x-ray pulse with peak power of a few hundred MW and duration shorter than the atomic unit of time can be generated from a 200 nm UV seed laser. It is capable of breaking the 24 as time barrier and may open a new regime of ultrafast sciences, such as realtime observation and control of atomic-scale electron dynamics, study of short-lived transit states for atoms and molecules, etc.

## ACKNOWLEDGEMENTS

We thank A. Chao, Y. Ding, D. Ratner, J. Wu and A. Zholents for helpful discussions. This work was supported by the U.S. Department of Energy under Contract No. DE-AC02-76SF00515.

## REFERENCES

- [1] P.M. Paul, *et al.*, Science 292, 1689 (2001).
- [2] E. Goulielmakis, *et al.*, Science 305, 1267 (2004).
- [3] M. Uiberacker, *et al.*, Nature(London) 446, 627 (2007).
- [4] F. Krausz and M. Ivanov, Rev. Mod. Phys, 81, 163 (2009).
- [5] E. Goulielmakis, *et al.*, Science 320, 1614 (2008).
- [6] E.L. Saldin, E.A. Schneidmiller, and M.V. Yurkov, Opt. Commun. 212, 377 (2002).
- [7] P. Emma, *et al.*, Phys. Rev. Lett, 92, 074801 (2004).
- [8] A.A. Zholents and W.M. Fawley, Phys. Rev. Lett, 92, 224801 (2004).
- [9] E.L. Saldin, E.A. Schneidmiller, and M.V. Yurkov, Opt. Commun. 239, 161 (2004).
- [10] A.A. Zholents and G. Penn, Phys. Rev. ST Accel. Beams, 8, 050704 (2005).
- [11] E.L. Saldin, E.A. Schneidmiller, and M.V. Yurkov, Phys. Rev. ST Accel. Beams, 9, 050702 (2006).
- [12] Y. Ding, *et al.*, Phys. Rev. ST Accel. Beams, 12, 060703 (2009).
- [13] A.A. Zholents and M.S. Zolotarev, New J. Phys, 10, 025005 (2008).
- [14] S. Reiche, P. Musumeci, C. Pellegrini and J.B. Rosenzweig, Nucl. Instrum. Methods Phys. Res., Sect. A 593, 45 (2008).
- [15] N.R. Thompson and B.W.J. McNeil, Phys. Rev. Lett, 100, 203901 (2008).
- [16] D. Xiang, Z. Huang and G. Stupakov, Phys. Rev. ST Accel. Beams, 12, 060701 (2009).
- [17] A. Zholents and G. Penn, These proceedings, (2009).
- [18] G. Stupakov, Phys. Rev. Lett, 102, 074801(2009).
- [19] D. Xiang and G. Stupakov, Phys. Rev. ST Accel. Beams, 12, 030702 (2009).
- [20] A. Baltuška, *et al.*, Nature(London) 421, 611 (2003).
- [21] Z. Huang and K. Kim, PAC'99, p. 2495 (1999).